



Deposited via The University of Sheffield.

White Rose Research Online URL for this paper:

<https://eprints.whiterose.ac.uk/id/eprint/90347/>

Version: Accepted Version

---

**Article:**

Ahmad, S., Kyriakides, N., Pilakoutas, K. et al. (2015) Seismic fragility assessment of existing sub-standard low strength reinforced concrete structures. *Earthquake Engineering and Engineering Vibration*, 14 (3). 439 - 452. ISSN: 1671-3664

<https://doi.org/10.1007/s11803-015-0035-0>

---

The final publication is available at Springer via <http://dx.doi.org/10.1007/s11803-015-0035-0>

**Reuse**

Items deposited in White Rose Research Online are protected by copyright, with all rights reserved unless indicated otherwise. They may be downloaded and/or printed for private study, or other acts as permitted by national copyright laws. The publisher or other rights holders may allow further reproduction and re-use of the full text version. This is indicated by the licence information on the White Rose Research Online record for the item.

**Takedown**

If you consider content in White Rose Research Online to be in breach of UK law, please notify us by emailing [eprints@whiterose.ac.uk](mailto:eprints@whiterose.ac.uk) including the URL of the record and the reason for the withdrawal request.

## Seismic fragility assessment of existing sub-standard low strength reinforced concrete structures

Sohaib Ahmad<sup>1†</sup>, Nicolas Kyriakides<sup>2‡</sup>, Kypros Pilakoutas<sup>1§</sup>, Kyriacos Neocleous<sup>1\*</sup> and Qaiser uz Zaman<sup>3\*\*</sup>

1. Dept. of Civil and Structural Engineering, University of Sheffield, UK

2. Dept. of Civil Engineering and Geomatics, Cyprus University of Technology, Cyprus

3. Dept. of Civil and Environmental Engineering, University of Engineering and Technology, Taxila, Pakistan

**Abstract:** An analytical seismic fragility assessment framework is presented for the existing low strength reinforced concrete structures more common in the building stock of the developing countries. For realistic modelling of such sub-standard structures, low strength concrete stress-strain and bond-slip capacity models are included in calibrating material models. Key capacity parameters are generated stochastically to produce building population and cyclic pushover analysis is carried out to capture inelastic behaviour. Secant period values are evaluated corresponding to each displacement step on the capacity curves and used as seismic demand. A modified capacity spectrum method is adopted for the degrading structures, which is further used to evaluate peak ground acceleration from back analysis considering each point on the capacity curve as performance point. For developing fragility curves, the mean values of peak ground acceleration are evaluated corresponding to each performance point on the series of capacity curves. A suitable probability distribution function is adopted for the secant period scatter at different mean peak ground acceleration values and probability of exceedance of limit states is evaluated. A suitable regression function is used for developing fragility curves and regression coefficients are proposed for different confidence levels. Fragility curves are presented for a low rise pre-seismic code reinforced concrete structure typical of developing countries.

**Keywords:** analytical fragility; damage index; non-engineered; brittle; variability; demand; capacity

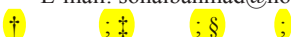
### 1 Introduction

The prediction of seismic damage potential of old and substandard reinforced concrete buildings is still a challenge for earthquake engineering community due to lack of damage data. However, with the improvements in different analytical tools and development of efficient analysis techniques, analytical procedures have been extensively used to derive fragility curves in the recent years. Both simple and detailed analytical methods exist in the literature for the derivation of fragility curves. The main difference between these methods lies in the sophistication used for the modelling of building. Simple methods do not require the analysis of structure, but rely on simple equations to derive its capacity. These

methods were derived with the objective of analysing a large number of buildings in a rather short period of time. Therefore, structural modelling is based on a few input parameters such as the period of construction, number of storeys and construction material.

Calvi (1999) proposed a simple analytical method based on the ratio between the displacement capacity of a building corresponding to several limit states and the displacement demand from an earthquake event as obtained from the corresponding displacement spectrum. A Displacement Based Earthquake Loss Assessment (DBELA) framework was developed by Pinho *et al.* (2002) and Crowley *et al.* (2004) for the analytical vulnerability assessment of Reinforced Concrete (RC) structures using the methodology of Calvi (1999). In contrast, the detailed analytical methods define capacity through analysis of the structural model, the sophistication of which varies based on the required accuracy. Detailed analytical procedures are more thorough and demanding, and are intended to be used when more detailed information is required, i.e. buildings with particular importance, structures for which no empirical data are available (innovative structural designs, sub-standard and low strength RC structures). Different researchers

**Correspondence to:** Sohaib Ahmad, Dept. of Civil and Structural Engineering, University of Sheffield, Sir Frederick Mappin Building, Mappin Street, S1 3JD, UK  
Tel: +44 (0)114 222 5071; Fax: +44 (0)114 222 5700  
E-mail: sohaibahmad@hotmail.com



Mosalam *et al.* (1997), Lang (2002), Gardoni *et al.* (2003), Franchin *et al.* (2003), Rossetto and Elnashai (2005), Erberik and Elnashai (2005), Erberik (2008), Celik and Ellingwood (2008) have developed fragility curves for the gravity loaded design (GLD) structures of developed countries by using detailed analytical approach. The type of method chosen in these studies for fragility analysis depends not only on the objective of the assessment, but also on the availability of data and technology. The accuracy of analytical fragility curves are found to be typically governed by the ground motion parameter, modelling assumptions, material models, response parameter, analysis techniques. However, the fragility curves developed in the existing studies do not give the detailed consideration of strength and stiffness degradation due to brittle failure modes (bond, shear etc.) and cannot be effectively used for the low strength non-engineered / pre-seismic code RC building stock of developing countries.

Analytical procedures based on nonlinear static analysis have now gained popularity due to efficiency and reliable results. Nonlinear static analysis was initially proposed in a number of design and assessment codes such as ATC-40 (1996) and FEMA356 (2000). In both cases, the capacity of the structure is expressed through the push-over capacity curve. In the former, the performance displacement is computed through highly damped spectra, whereas in the latter the displacement coefficient method is used as a simple alternative. An attempt to improve these methods was made in FEMA440 (2005). In particular for the ATC-40 (1996) method, a considerable improvement was achieved and eventually the method was substituted by the modified acceleration-displacement response spectrum (MADRS) procedure. Rossetto and Elnashai (2005) used a modified capacity spectrum method (CSM) for evaluating seismic demand in terms of  $ISD_{max}$ . Adaptive pushover analysis and performance specific spectra were used to define capacity and demand, respectively.

Among many vulnerability studies very few tried to incorporate the effect of degrading brittle behaviour. When dealing with sub-standard RC buildings, modelling of the structure should be able to accommodate a number of failure modes such as flexure, shear, local buckling and debonding of reinforcement. It should be noted that most analytical vulnerability studies concentrate primarily on the flexural and, to a smaller extent, shear or bond failures at the member level (Dymiotis *et al.*, 1999; Rossetto and Elnashai, 2005; Ahmed, 2006). Erberik (2008) evaluated the fragility of low and mid-rise RC structures (bare and in-filled) in Turkey. To incorporate the degrading behaviour, an energy based hysteretic model that accounts for a two parameter low cycle fatigue model was used. One parameter controls the level of degradation and the other controls the rate of degradation. Three types of building degradation levels were considered ranging from theoretically no degradation to very high degradation of brittle

structures. In another research, Celik and Ellingwood (2008) studied the importance of modelling the shear and bond-slip behaviour of the beam-column joints for the fragility analysis of GLD RC frame structures of the mid-American region. In this study, the full scale beam-column joints cyclic test data from existing research were used to select appropriate joint model to attain the realistic joint shear stress-strain relationship. Dipasquale and Cakmak (1988), Calvi *et al.* (2006) and Zembaty *et al.* (2006) have found period elongation of RC structure to be good representative of global structural damage accumulation and is recommended as a good damage index. Kyriakides *et al.* (2014) developed a framework for the analytical seismic vulnerability assessment of substandard RC structure using improved modelling assumptions, utilizing probabilistic techniques and improving the performance evaluation method for RC structures. A simple methodology to model the complex degradation behaviour of brittle structures was proposed and used in the framework. Moreover, a damage index based on secant period is used to quantify damage at different PGA levels. The vulnerability curves gives damage in terms of percentage at different PGA levels.

Different approaches to develop fragility functions using seismic demand data have been reported in literature. Singhal and Kiremidjian (1997) used "stripe" analysis, whereas a "cloud" analysis was carried out by Cornell *et al.* (2002) using all the seismic demand data. Celik and Ellingwood (2010) and Erberik (2008) have used the stripe analysis for generating the damage distributions. A demand model was defined in the existing studies having median seismic demand which was presented as a log-linear function of a ground motion parameter. It was assumed that about the median, the structural demand is log-normally distributed having a constant logarithmic standard deviation. Ramamoorthy *et al.* (2006) established a bilinear relationship (instead of linear as used by Cornell *et al.*, 2002) for median seismic demand. A Bayesian relationship was used to evaluate the regression parameters of the demand model.

This paper presents an extended framework for carrying out probabilistic analytical fragility assessment of existing low-rise and low strength RC structures more common in the building stock of developing countries. The methodology was based on considering the improved modelling assumptions, use of new capacity models for low strength concrete (LSC), bond and incorporating improved performance evaluation method for brittle structures. The capacity related uncertainties are addressed probabilistically. The degradation effects due to bond and shear are addressed by conducting cyclic pushover analysis. Secant period is used as a seismic demand parameter and the performance planes corresponding to limit states from literature are identified to evaluate probability of exceedance. Fragility curves for low rise structure with different design categories are derived as a function of mean peak ground acceleration using a suitable distribution and a regression function.

## 2 Description of the flowchart for the proposed seismic fragility assessment framework

The flowchart diagram for the proposed probabilistic analytical seismic fragility assessment framework is presented in Fig. 1. Steps 13 to 17 are the additions in existing framework by Kyriakides *et al.* (2014) to derive suitable regression function and the regression coefficients for developing fragility curves of low-rise and low strength sub-standard RC structures of developing countries.

- In Step 1, the building category to be examined is defined.
- In Step 2, the key capacity parameters and their variabilities are selected, and explained in Section 3.3.
- To limit the number of simulations, the latin hypercube sampling (LHS) technique is used in Step 3 to generate the variables  $P_{ij}$  (see Step 4) for the analysis.
- Based on the properties of the  $P_{ij}$  variables, the capacities and other required inputs are evaluated to calibrate the material and hysteretic models in Step 4.
- The structural model for a particular building

category with the required inelastic elements is developed in Step 5.

- The building population with different characteristics is generated for a single analysis in Step 6. The inelastic elements of the structural models are calibrated using outcomes of Step 4.
- In Step 7, cyclic analysis is undertaken for building population to produce the capacity envelopes with displacement ( $u$ ) vs base shear ( $bs$ ) as output.
- Process 8 transforms the capacity curves into spectral acceleration (SA) and spectral displacement (SD).
- Step 9 evaluates the secant period ( $T_{sec}$ ) corresponding to each point, using Eq. (6) as shown in Fig. 3.
- Step 10 selects the type of energy balance of each defined equivalent system as discussed in Section 3.1. This leads to the evaluation of ductility ( $\mu$ ) and initial period ( $T_{ini}$ ) of each system.
- Step 11 evaluates the  $T_{eff}$  and  $\beta_{eff}$  according to FEMA440 (2005) provisions.
- Step 12 evaluates the reduction factors  $\eta$  and  $M$

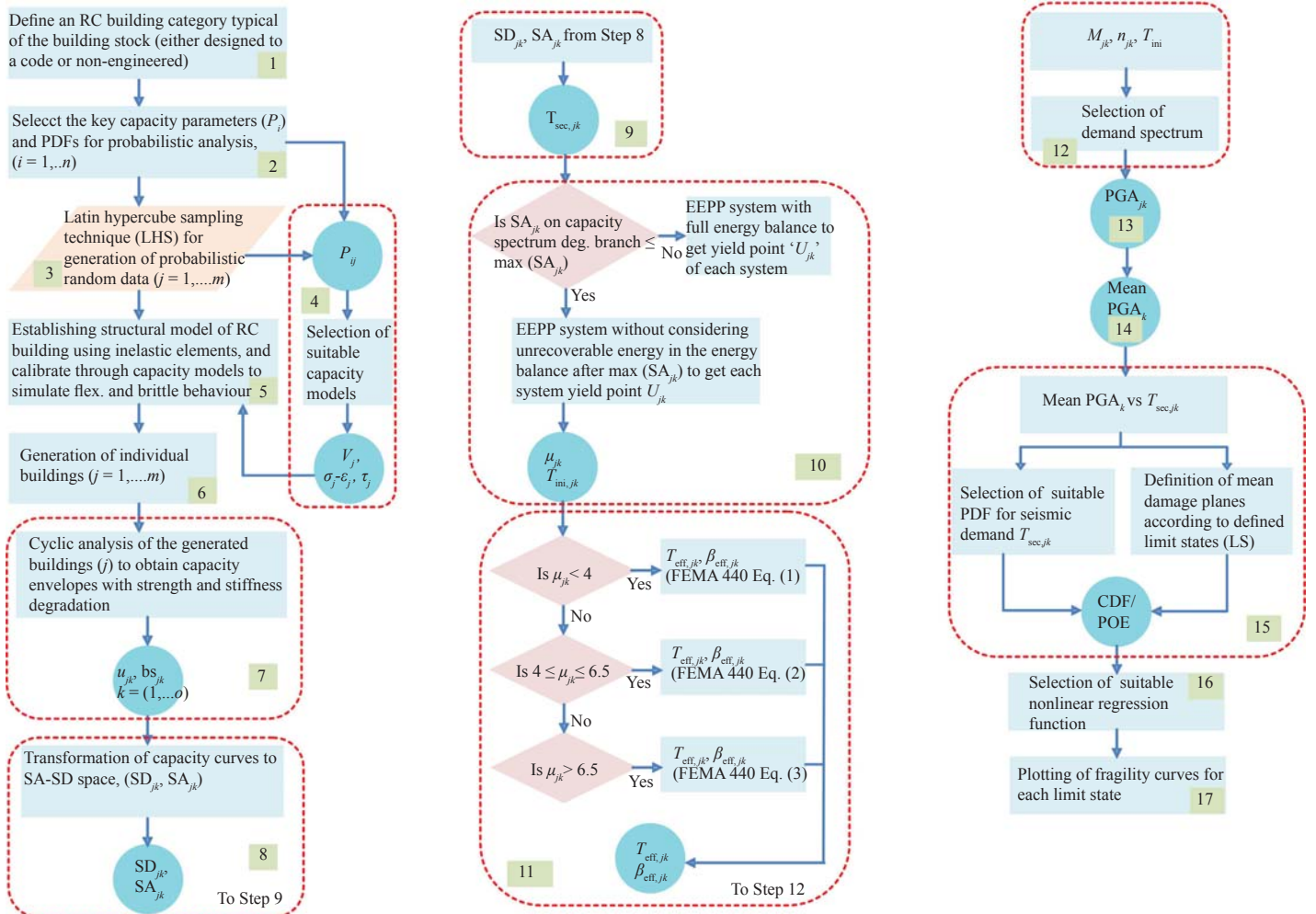


Fig. 1 Proposed framework for the probabilistic analytical seismic fragility assessment of low strength RC structures

according to FEMA440 (2005).

- Step 13 uses the EC8 spectrum relationship for Peak Ground Acceleration ( $PGA_{jk}$ ) calculation using the process defined in Section 3.2.

- The mean  $PGA_k$  is evaluated from  $PGA_{jk}$  corresponding to each performance point of the series of capacity curves in Step 14.

- In Step 15, the suitable probability distribution function (PDF) is chosen for the  $T_{secjk}$  data at each mean  $PGA_k$  value and the cumulative distribution function (CDF) is evaluated. probability of exceedance (POE) is evaluated and the scatter for each limit state is extracted.

- A suitable regression function is adopted in step 16 for developing fragility curves.

- Step 17 involves plotting of the fragility curves for different limit states.

### 3 Description of the framework's critical procedures

#### 3.1 Modelling complex degradation behaviour of non-ductile equivalent systems

To address the issue of modelling complex degradation behaviour, the method proposed by Kyriakides *et al.* (2014) is used. In this method, the use of a single strength and stiffness  $E-P$  approximation in FEMA 440 (2005) is considered insufficient to capture the more complex degrading behaviour encountered in sub-standard constructions. Therefore, in order to maintain the special characteristics of the capacity curve it is proposed that the shape of curve is approximated by a number of different elastic-perfectly plastic systems with zero post-yield stiffness as shown in Fig. 2(a). Each  $SA_i-SD_i$  coordinate on capacity curve is treated as the strength and ultimate displacement of an equivalent

elastic-perfectly plastic system (EEPP) defined using the equal energy rule. However, after degradation, energy dissipated above the current force level is considered unrecoverable and is excluded from the energy balance calculation (Fig. 2(b)). Therefore, the proposition for idealisation of the capacity curve is based on its discretization into a number of performance points (PP's) each corresponding to a single EEPP system.

Figure 3(a) shows the cumulative area under the capacity curve at  $SD(j)$  corresponding to the maximum capacity point. EEPP corresponding to this point is shown in Fig. 3(b). The equal area rule is applied to evaluate the yield displacement  $U(j)$  using Eq. (1).

$$U(j) = -\frac{2(C_{area}(j) - (SD(j)SA(j)))}{SA(j)} \quad (1)$$

The performance of the proposed idealisation procedure was assessed numerically in predicting the seismic demand of a range of brittle low strength structures. The EEPP method when used along with FEMA 440, MADRS gave less error in seismic demand predictions as compare to the FEMA440, MADRS method when used with the bilinearization technique having post elastic stiffness. Full details of this study is given in Kyriakides (2008) and Ahmad (2011).

#### 3.2 Calculation of peak ground acceleration (PGA)

The modified capacity-spectrum method can be implemented in a reverse manner (back analysis) to estimate the PGA corresponding to each point ( $SA_r, SD_r$ ) on the capacity curve which is treated as a PP. For that purpose, the capacity-spectrum method (MADRS) proposed in FEMA440 (2005) is used along with EEPP method. The multiple performance points ( $SA_r, SD_r$ ) assumption and equivalent systems on the capacity

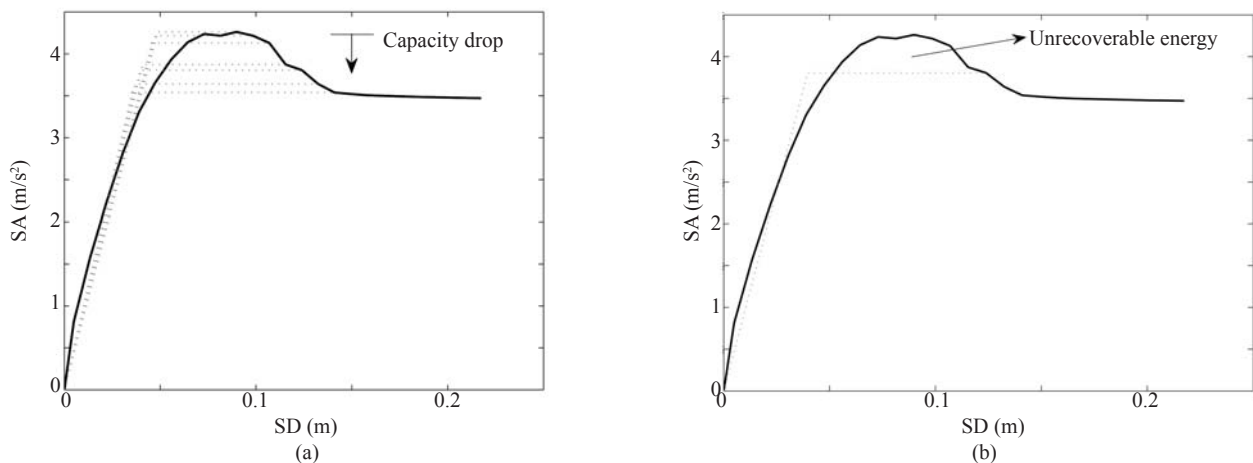
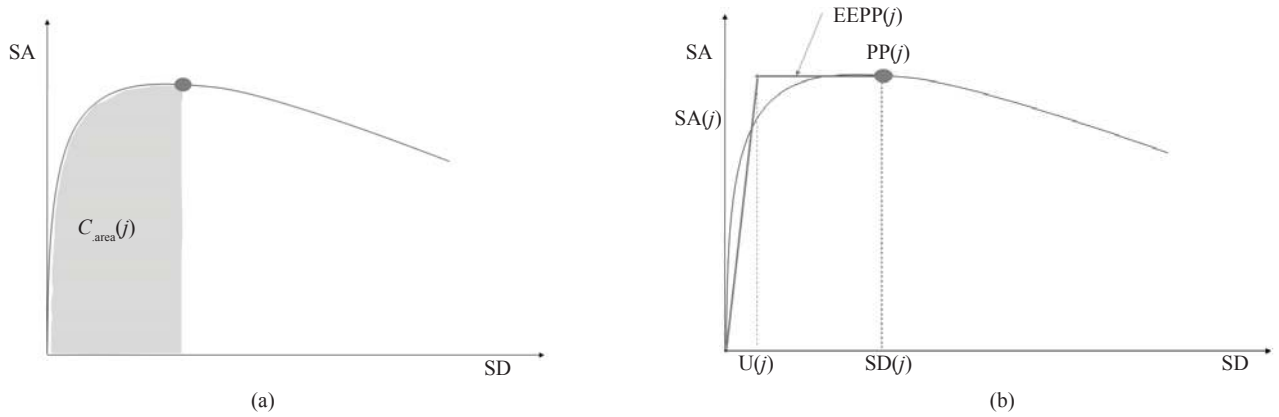


Fig. 2 Modelling of complex degradation behavior using EEPP method (a) Series of EEPP systems corresponding to each performance point on capacity curve with strength and stiffness degradation (b) Unrecoverable energy at higher displacement after degradation, (Kyriakides *et al.*, 2014)



**Fig. 3** Evaluation of yield displacement for EEPP (a) Cumulative area at a particular spectral displacement (b) Implementation of equal energy rule for yield displacement evaluation using the proposed methodology

curve (described in Section 3.1) are first used to evaluate  $T_{eff}$  and  $\beta_{eff}$  corresponding to the ductility (from Eq. (1)) at each PP. Subsequently,  $\beta_{eff}$  is substituted in the (EC8) elastic spectrum equation to calculate the reduced acceleration-displacement response spectrum (ADRS) with increased damping ( $\beta_{eff}$ ). To finalise the reduction of the spectrum, each ordinate of  $SA_i$  on the ADRS is multiplied by a factor  $M$  to generate the modified ADRS (MADRS) spectrum (Fig. 4). Factor  $M$  corresponds to the difference in ductility between the nonlinear ( $T_{sec}$ ) and “equivalent” linear ( $T_{eff}$ ) SDOF systems.

MADRS spectrum relation evolved from EC8 response spectrum relation is used to estimate the PGA at each PP (Fig. 5) from the back analysis by using Eq. (2). Mean PGA values are further calculated from the PGA values associated with the same PP’s on different capacity curves of building population (Fig. 5) using Eq. (3), which is later used in developing fragility curves.

$$PGA(jk) = \frac{SA(jk)T_{ini}(jk)}{\alpha SM(jk)\eta(jk)T_c} \quad (2)$$

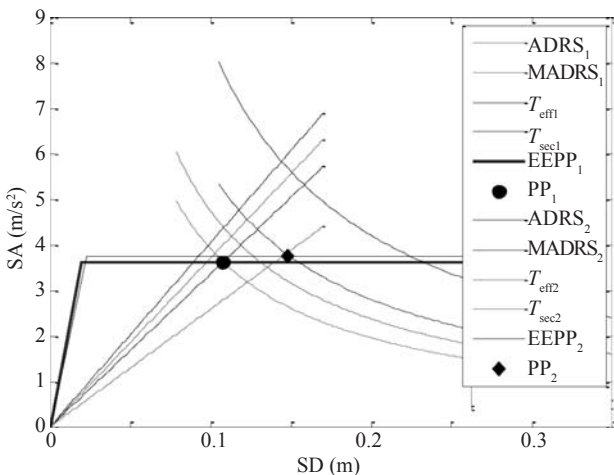


**Fig. 4** Reverse MADRS method with representative EEPP systems for PGA calculation

$$meanPGA(k) = \frac{\sum_{j=1}^m PGA(jk)}{m} \quad (3)$$

where

- $j$  = building population
- $k$  = a performance point on capacity curve
- $m$  = total number of buildings
- $SA$  = spectral acceleration
- $T_{ini}$  = initial period of the equivalent system
- $T_c$  = site characteristic period
- $A$  = spectral amplification coefficient
- $S$  = soil factor
- $\eta$  = reduction factor
- $M$  = modification factor

The advantage of using back analysis for PGA calculation is the consideration of demand uncertainty in an indirect manner. This is quicker than using time history analysis, where a lot of artificial or natural ground motion record sets corresponding to different

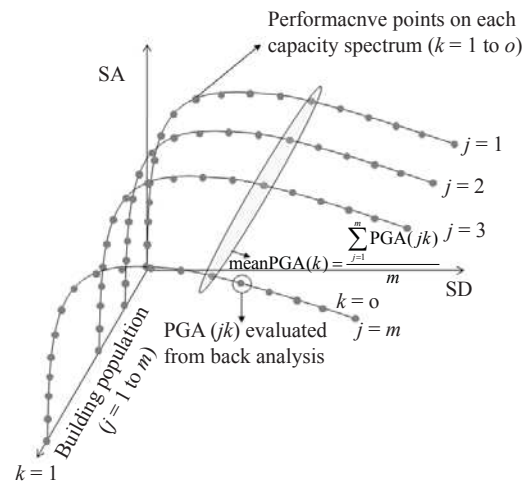


**Fig. 5** Schematic representation of the PGA and mean PGA calculation from PP’s on building population capacity spectra

PGA levels are required. Moreover, the PGA evaluated by this method is also performance consistent for a particular category of structures.

### 3.3 Variability of capacity parameters for analytical fragility curves

In order to study the probabilistic aspect of the analytical fragility curves, the variability of the various key capacity parameters involved in the calibration of material models needs to be accounted for. This is essential in order to account for variations and uncertainty in design and detailing of buildings of the same type and construction period. The main source of variability comes from parameters involved in the calibration of the capacity models of the main RC structural members (beams and columns). The capacity models influencing the structural response of the members are the flexural, shear and bond models. The parameters involved in their calibration can be divided into three broad categories, which include strength-related, geometrical and design parameters as shown in Table 1. The variability of strength-related parameters can be addressed using either expert judgement, code provisions or by using available statistics so as to set the basis for the generation of the probability density function (PDF). These strength-related parameters are regarded as the key probabilistic

**Table 1 Calibration parameters for capacity models**

Capacity model	Key parameters	Deterministic parameters	Design parameters
Flexure:	$f_y, f_c$	$b, d, k = f_{ult}/f_y, \epsilon_{su}$	$\rho$
Shear:	$f_c, s$	$b, d, f_{yw}$	$A_{sw}, s$
Bond:	$f_{ct}, s, l, c$		$s, l, d_b$

where:

- $f_c$  = concrete compressive strength
- $f_y$  = steel yield strength
- $s$  = shear link spacing
- $f_{ct}$  = concrete tensile strength
- $l$  = anchorage length
- $c$  = concrete cover
- $d_b$  = longitudinal bar diameter
- $d_{bw}$  = shear link bar diameter
- $f_{yw}$  = shear link yield strength
- $b, d$  = section dimensions
- $\rho$  = longitudinal reinforcement ratio
- $\epsilon_{su}$  = strain in steel at ultimate steel stress

parameters and PDF parameters used for the generation of probabilistic fragility curves are given in Table 2.

The simulation values are obtained using the corresponding PDF using the Latin Hypercube Sampling algorithm. This technique, proposed by McKay *et al.* (1979) enables the reduction in the number of simulations compared to the Monte Carlo technique by adopting a stratified approach in selecting the simulation values from the PDF. Initially it is assumed that each key parameter is uniformly distributed in the space between 0 and 1. The uniform distribution is divided into a number of non-overlapping sub-intervals equal to the number of simulations. A uniform value  $U_i$  is then selected at random from each sub-interval (Eq. (4)) and the inversion method is applied to transform them into values that correspond to the cumulative distribution function (CDF) of each key parameter.

$$U_i = \frac{(\pi_i - 1) + u_i}{N} \quad (4)$$

where:

$N$  is the number of simulations;  $\pi_i$  is random permutations of the integers  $i = 1, \dots, N$ ;  $u_i$  is the uniform random numbers on  $[0, 1]$  generated independently from  $\pi_i$ .

Rossetto and Elnashai (2005) and Kyriakides *et al.* (2012) used 25 simulations in their studies. However, due to the inclusion of additional parameters ( $L_d(d_b), c(d_b)$ ) in the current study, 50 simulations were found to lead to convergence and are used for each building to account for uncertainty in the response of low strength RC structures.

### 3.4 Secant period calculation

Time period elongation is considered to be the global parameter of damage by many researchers (Calvi *et al.*, 2006; Zembaty *et al.*, 2006). In the current study, secant period ( $T_{sec}$ ) is evaluated corresponding to each PP on the capacity envelopes of degrading cyclic response of structures by using Eq. (5). This represents damage level or seismic demand corresponding to a mean PGA (Eq. (3)).

$$T_{sec} = 2\pi \sqrt{\frac{SD_i}{SA_i}} \quad (5)$$

**Table 2 Probabilistic data of key parameters used for fragility analysis**

	Parameter	Probability density function	Mean ( $\mu$ )	Standard deviation ( $\sigma$ )	Minimum value	Maximum value
Pre-seismic	$f_c$ (MPa)	Log-normal	8	11	$\mu - 0.3\sigma$	$\mu + 1.5\sigma$
	$f_y$ (MPa)	Normal	325	30	$\mu - 2\sigma$	$\mu + 2\sigma$
	$L_d(d_b)$	Normal	10	2	$\mu - 2\sigma$	$\mu + 2\sigma$
	$c(d_b)$	Log-normal	1	1	$\mu - 0.5\sigma$	$\mu + 0.5\sigma$
	$s$ (mm)	Normal	280	20	$\mu - 3\sigma$	$\mu + 3\sigma$

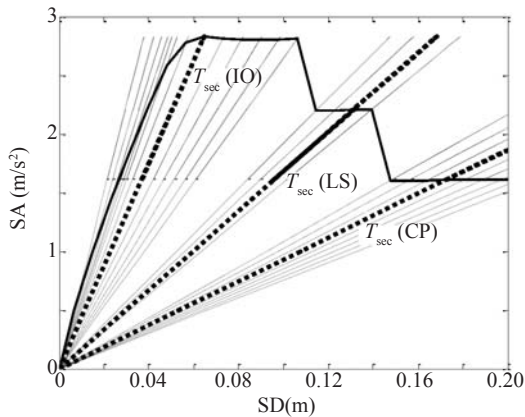


**Fig. 6** Secant periods radial planes corresponding to each performance point and three limit states

where

$SD_i$  = spectral displacement at point ‘i’ on capacity curve

$SA_i$  = spectral acceleration at point ‘i’ on capacity curve

All secant period values related to the capacity curve are shown by the radial lines in Fig. 6 and represents performance planes. For a fragility curve development, multiple intermediate performance planes corresponding to different limit states can be defined. The drift threshold values associated with different limit states can be found in various codes, which can be used to evaluate their corresponding secant period. For the current study, three secant period planes (Fig. 6) corresponding to FEMA 356 (2000) limit states (Immediate Occupancy (IO), Life Safety (LS), Collapse Prevention (CP)) are used to evaluate their probability of exceedance (POE) at a particular PGA level.

#### 4 Application of the framework

The remaining of the paper focuses on the application of the seismic fragility framework on a low strength case building. To demonstrate the framework, DRAIN 3DX (Prakash *et al.*, 1994) was selected as the analytical tool due to the availability of suitable inelastic elements in its library to realistically simulate the degradations (particularly due to bond deterioration and shear strength degradation) in the response of brittle structures. The selected RC building type, material/capacity models are discussed in Section 4.1 and 4.2, respectively.

##### 4.1 Building selection for fragility assessment

A very large array of low and mid rise building categories over different construction and design periods (CDP) can be examined. To illustrate the proposed framework, seismic fragility curves are generated for low rise (LR) RC buildings of a single CDP (pre-seismic design codes). Pre-seismic category structures refers to GLD moment resisting frames (MRF) with no seismic

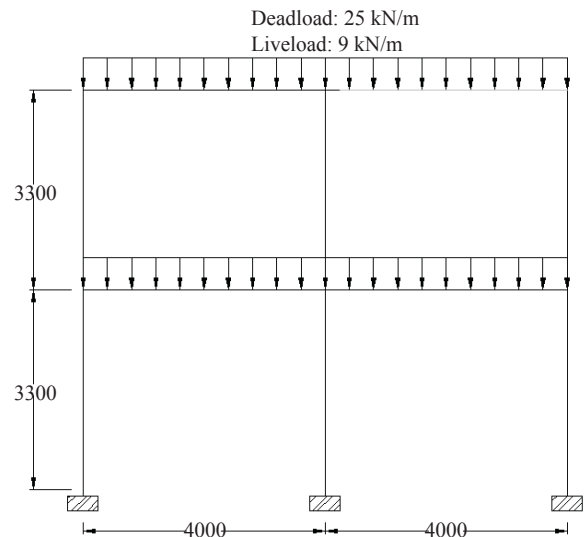
design consideration. Moreover, deficiencies commonly found in the low strength RC structures of developing countries because of the use of poor quality materials insufficient anchorage and detailing are also accounted for.

A 2 storey 2 bay structure typically used for commercial or residential purposes is chosen, as shown in Fig. 7. There can be a number of different design sub-categories and configurations, but three typical design sub-categories and a bare frame with regular configuration are chosen as an example. These design sub-categories were chosen to reflect the variation in section geometry of beams and columns, which may lead to the weak column-strong beams effect. The beam and column section details corresponding to each design sub-category is given in Table 3.

A random building population was generated using the PDF parameters for the key (strength-related) capacity parameters through LHS. Due to the random assignment of the capacity parameters, each sub design category can have brittle (e.g. bond or shear failure) or flexural failure mode and thus the derived fragility curves cover the broad spectrum of poorly constructed buildings in many developing countries.

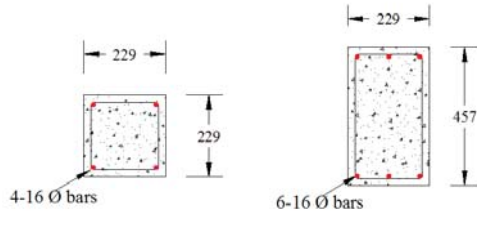
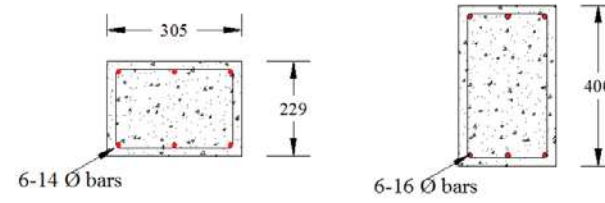
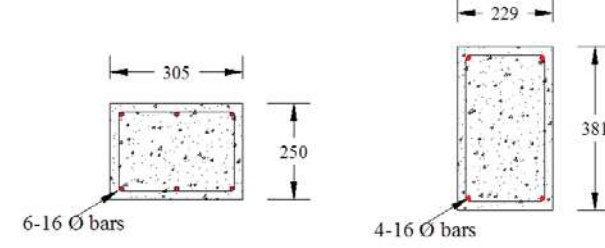
##### 4.2 Material and capacity model for analysis

Modelling of frame members in DRAIN 3DX was done using fiber element (element 15). The calibration of the material model for concrete was conducted using the low strength concrete (LSC) stress-strain ( $\sigma$ - $\epsilon$ ) material model by Ahmad *et al.* (2014) by defining five  $\sigma$ - $\epsilon$  points. This LSC  $\sigma$ - $\epsilon$  model is given in Eq. (6). This is modified Mander model, which as compare to the original Mander model (Mander *et al.*, 1988) has extra ‘ $\alpha$ ’ variable for low strength concrete given in Eq. (7). The ‘ $\alpha$ ’ variable is obtained after calibrating the Mander model using the LSC  $\sigma$ - $\epsilon$  experimental data.



**Fig. 7** LR building for seismic fragility assessment (2 storey 2 bay regular bare frame)

**Table 3** Beam and column section details of different sub-design categories of pre-seismic design period

Sr. No.	Pre-seismic	
	Column	Beam
1	Sub-design 1	
2	Sub-design 2	
3	Sub-design 3	

$$f_c = \frac{f'_c x r}{r - 1 + x^{\alpha}} \quad (6)$$

$$\alpha = \left( \frac{f'_c + 23}{38} \right)^{0.45} \quad (7)$$

where

$$x = \frac{\varepsilon_c}{\varepsilon'_c}, \quad r = \frac{E_c}{E_c - E_{sec}}$$

$$E_c = 5000\sqrt{f'_c}, \quad E_{sec} = \frac{f'_c}{\varepsilon'_c}$$

$\varepsilon_c$  = strain at any stress point in a stress-strain curve

$f'_c$  = unconfined concrete compressive strength (MPa)

$E_c$  = elastic modulus of concrete (MPa)

$E_{sec}$  = secant modulus of concrete corresponding to  $f'_c$

$\varepsilon'_c$  = peak strain of unconfined concrete

The representative LSC  $\sigma$ - $\varepsilon$  curve ( $f'_c = 7$  MPa) and steel bilinear  $\sigma$ - $\varepsilon$  curve ( $f_y = 290$  MPa) example used for calibrating the material models in DRAIN 3DX are given in Figs. 8(a) and (b), respectively.

To incorporate the effect of bond-slip ( $\tau$ - $s$ ) behaviour in the analysis, connection hinges (Element 15) were also used at the joints. The hinges comprising of fibres

were used to model both the pullout and gap effects. These hinges were located at the element ends, where the steel is replaced by pullout fibres and the concrete by gap fibres. To model the characteristics of a pullout hinge, a monotonic tri-linear envelope is needed and a stress-displacement envelope should be defined both in tension and compression. The LSC bond strength model by Ahmad (2011) and a suitable assumption for the strain distribution were used to model the  $\tau$ - $s$  behaviour. To evaluate the initial bond stiffness, a uniform strain distribution (Fig. 9(a)) was assumed over the embedment length and Eq. (8) was used to define the elastic slip. For post yield, a linear strain distribution is assumed after yielding as shown in Fig. 9(b) and Eq. (9) was used to evaluate the plastic slip.

when  $f_s \leq f_y$

$$\text{Slip} = \frac{f_s^2 d_b}{8E_s \tau_c} \quad (8)$$

when  $f_s > f_y$

$$\text{Slip} = \frac{f_y^2 d_b}{8E_s \tau_c} + \frac{(f_s - f_y) f_y d_b}{4\tau_y E_s} + \frac{(f_s - f_y)^2 d_b}{8\tau_y E_h} \quad (9)$$

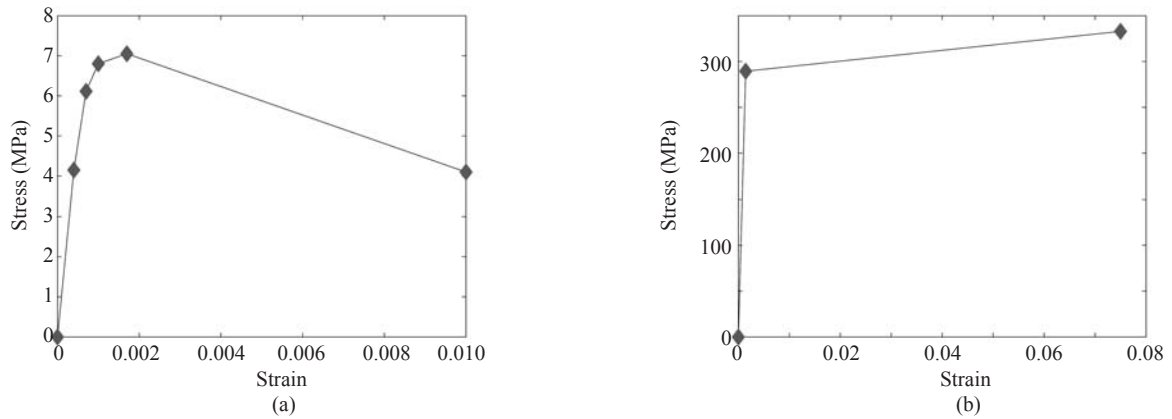


Fig. 8 Example of stress-strain ( $\sigma$ - $\epsilon$ ) models for calibrating Drain 3DX material models (a) LSC  $\sigma$ - $\epsilon$  model (b) Steel  $\sigma$ - $\epsilon$  model

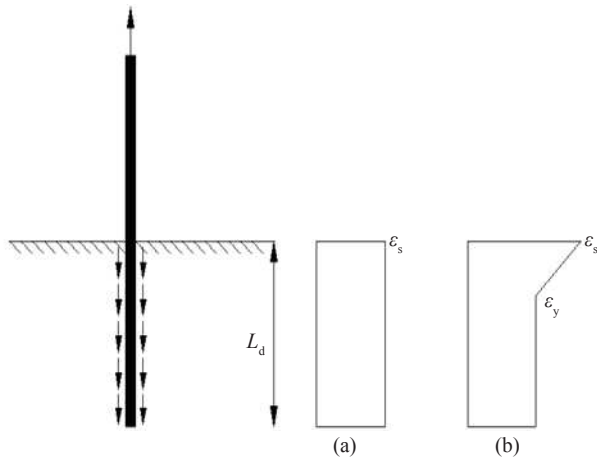


Fig. 9 Strain distributions for different conditions (a) up to yield (b) post yield case

where

- $\tau_e$  = elastic bond strength
- $\tau_y$  = yielded bond strength
- $d_b$  = steel bar diameter
- $f_s$  = bar stress
- $f_y$  = yield strength of bar
- $E_h$  = steel hardening modulus
- $E_s$  = steel modulus of elasticity

The choice of appropriate shear capacity model is very important for the assessment of deficient structures. The Sezen and Moehle (2004) relation (Eq. (10)) was used to evaluate the shear capacity. The ductility factor 'k' is applied to both the steel and concrete contribution since the contribution of concrete and steel to shear degradation is assumed to be equally significant. The value of 'k' between 1 and 0.7 is related linearly to ductility levels of 2 to 6. Element 8 of DRAIN 3DX was used to model the shear behaviour of the joint.

$$V_n = V_s + V_c = k \left( \frac{A_v}{s} f_y d \right) + k \left( \frac{0.5\sqrt{f_c}}{a/d} \sqrt{1 + \frac{P}{0.5\sqrt{f_c} A_g}} \right) 0.8A_g \quad (10)$$

where

- $P$  = axial force
- $k$  = ductility related strength degradation value
- $a/d$  = aspect ratio
- $A$  = cross-sectional gross area
- $A_g$  = shear link area
- $f_y$  = yield strength of steel
- $f_c$  = concrete compressive strength

The representative Drain 3DX model with various in-elastic elements for simulating sub-design 1 category building flexural / brittle response is shown in Fig. 10.

The cyclic pushover capacity envelopes representative of the three sub-design categories (Table 3) are shown in Figs. 11(a)-(c). These envelopes show strength and stiffness degradations of the case structure due to inclusion of connection and shear hinges and use of adequate capacity models for calibration.

## 5 Fragility curves

As mentioned previously (Section 3), capacity curves and the different secant period damage planes corresponding to defined limit states are used to derive fragility curves. For the current study, three secant period damage planes corresponding to the limit states (IO, LS, CP) of FEMA 356 (2000) are used to evaluate the POE of a damage state at a particular ground motion level. The PGA corresponding to each PP of the stochastically generated capacity curves are determined using the same back analysis procedure (Section 3.2) and the mean PGA values are evaluated.  $T_{sec}$  is used as a seismic demand parameter for defining statistical distributions over the mean PGA values and is assumed to be normally distributed. The plots of mean PGA vs  $T_{sec}$  for each design sub-category are shown in Figs. 12(a)-(c). The three limit states in terms of secant period calculated using Eq. (5) are also shown in the Figs. 12(a)-(c).

In the proposed method, there is no need to undertake either stripe or cloud analysis as done by many researchers in their fragility assessment studies. The POE of each damage state at different PGA levels

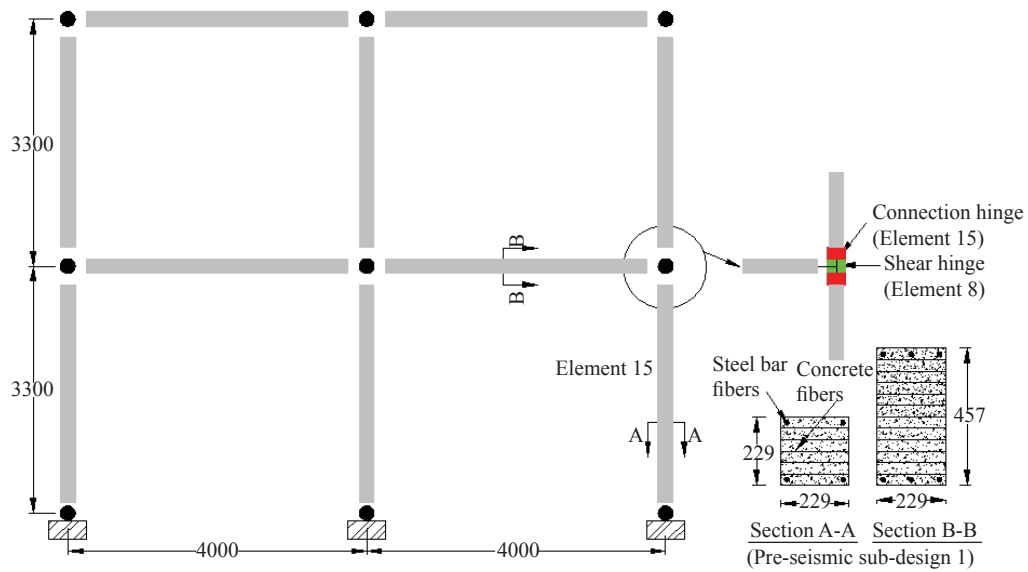


Fig. 10 Drain 3DX model of Sub-design 1 category frame with different in-elastic elements for cyclic pushover analysis

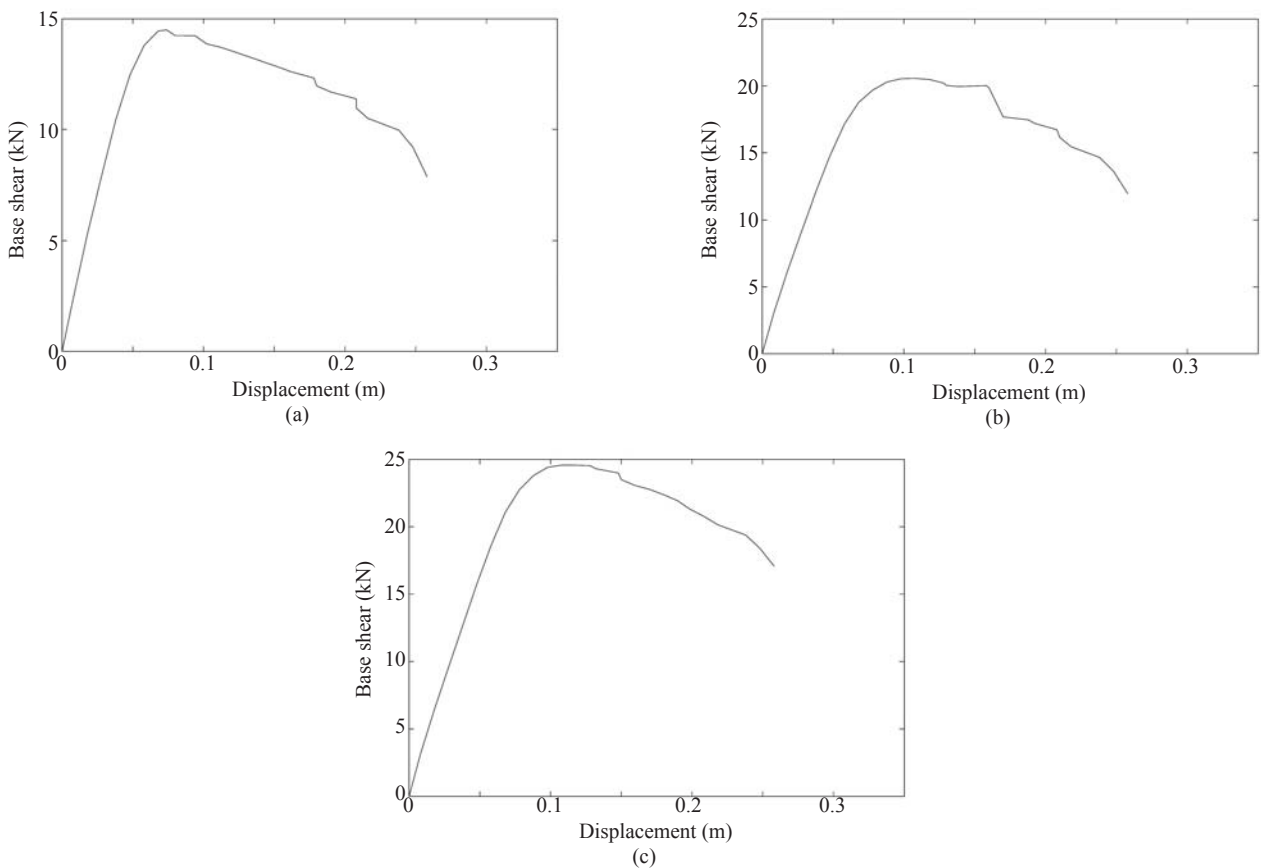
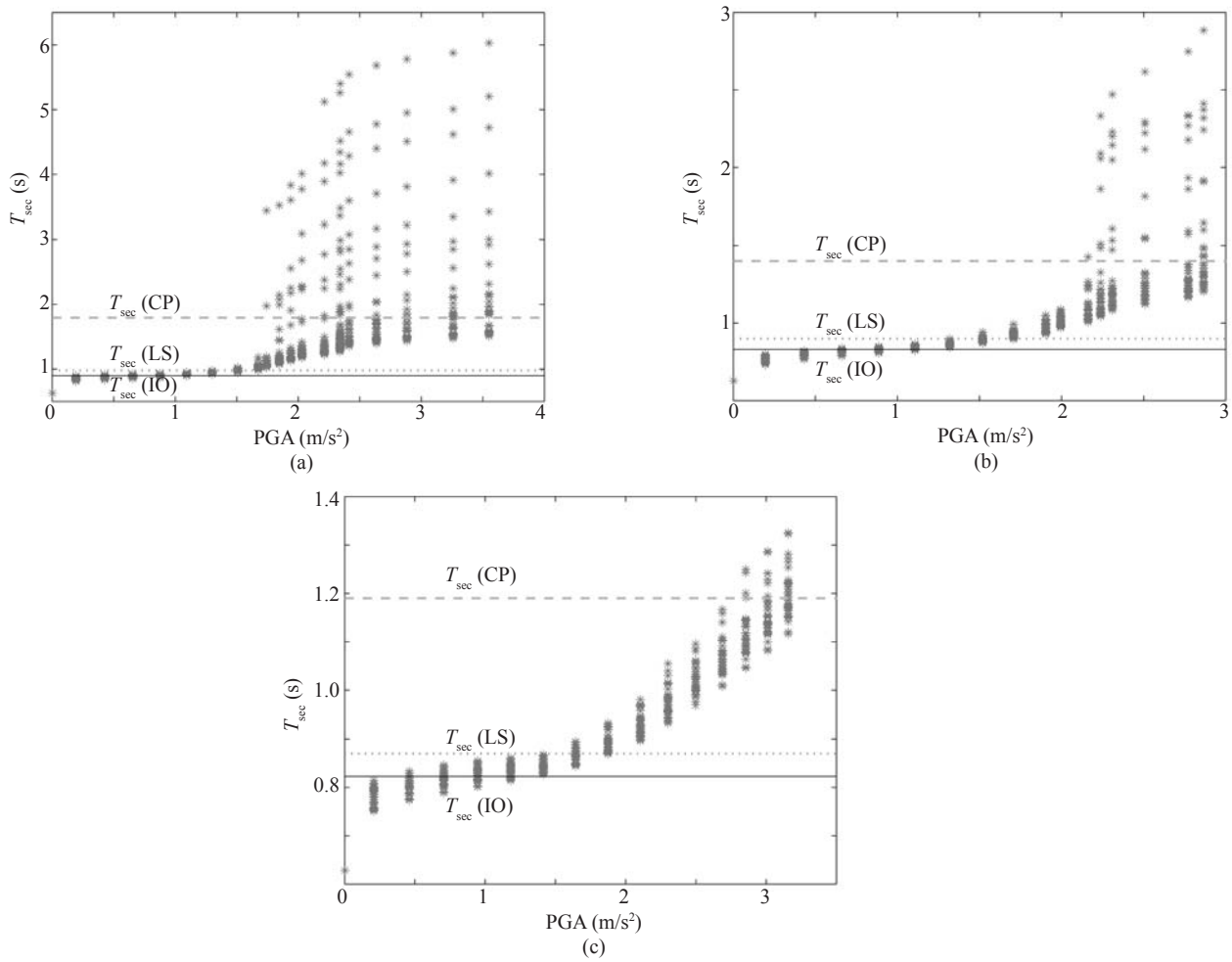


Fig. 11 Representative cyclic pushover capacity envelopes with degradation (a) Sub-design 1 (b) Sub-design 2 (c) Sub-design 3

are evaluated using the cumulative distribution function. This is given by Eq. (11) and Eq. (12).

$$F_i(\text{PGA}) = P(D > d_i / \text{GM} = \text{PGA}) \quad (11)$$

where;  $F_i(\text{PGA})$  is the POE of damage  $D$  from damage state  $d_i$  at a given ground motion  $\text{GM} = \text{PGA}$ . Damage states  $i$  are defined from the non-damage state ( $i = 0$ ) to the  $n$ th damage state ( $i = n$ ).  $d_{it}$  is the threshold values of



**Fig. 12**  $T_{sec}$  scatter of substandard pre-seismic building population over mean PGA for fragility curve generation (a) Sub-design 1 frame (b) Sub-design 2 frame (c) Sub-design 3 frame

damage states.  $f_{im}(d_i)$  is the PDF of  $T_{sec}$  and  $F(d_{it})$  is the CDF at every PGA, respectively.

$$\begin{aligned}
 F_i(\text{PGA}) &= P(D > d_{it} / \text{GM} = \text{PGA}) \\
 &= 1 - F(d_{it}) = 1 - \int_{-\infty}^{d_{it}} f_{im}(d_i) d(d_i)
 \end{aligned}
 \quad (12)$$

The function given in Eq. (13) is used to fit the fragility curves on the POE data (corresponding to three performance levels) through nonlinear regression analysis.

$$P(d \geq DI / \text{GM}) = 1 - \exp(-\alpha \text{GM}^\beta) \quad (13)$$

where, GM represents a variety of ground motion parameters (PGA,  $S_{a5\%(\text{Telastic})}$ ,  $S_{d5\%(\text{Telastic})}$ ,  $S_{a0\%(\text{Inelastictic})}$ ) and  $\alpha$  and  $\beta$  are function shape parameters derived from

nonlinear regression on the damage data in each dataset. The framework for developing fragility curves is already given in Fig. 1 and the outcomes are presented in the following.

The  $T_{sec}$  scatter corresponding to mean PGA values (Fig. 12) for each sub-design category represents damage in sub-standard pre-seismic buildings distributed over different PGA levels. This scatter is further analyzed according to the procedure defined above to develop fragility curves for three limit states. The fragility curves for each sub design category of substandard / pre-seismic CDP are shown in Figs. 13(a) - (c). Mean fragility curves termed as general fragility curve for the three sub-design categories are also developed for three limit states and are shown in Fig. 14. The mean values of the coefficients after the nonlinear regression are given in Table 4 for the general curves. Moreover, confidence bounds (90% confidence interval) are also predicted for these mean fragility curves and are given in Table 4.

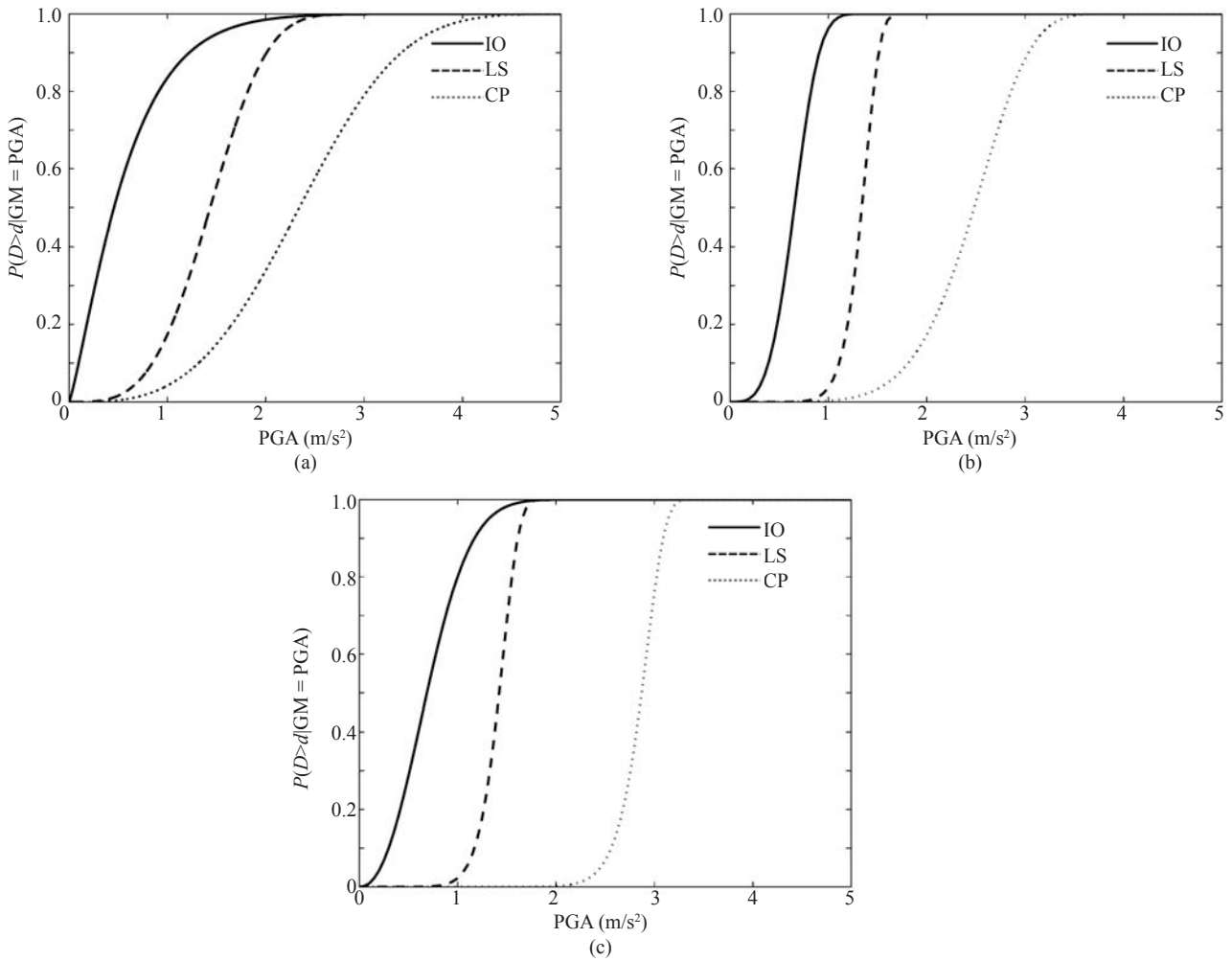


**Fig. 13** Fragility curves for substandard pre-seismic low rise RC buildings (a) Sub-design 1 frame (b) Sub-design 2 frame (c) Sub-design 3 frame

**Table 4** Coefficients for generation of mean and 90% confidence fragility curves for low rise RC buildings

Coefficients	General curve (pre-seismic) coefficients for different damage states (IO, LS, CP)								
	Mean			Lower bound			Upper bound		
	IO	LS	CP	IO	LS	CP	IO	LS	CP
$\alpha$	1.8	0.41	0.021	1.78	0.30	0.0301	1.26	0.52	0.0241
$\beta$	0.85	1.92	4.26	0.75	1.51	3.25	0.95	2.32	5.28

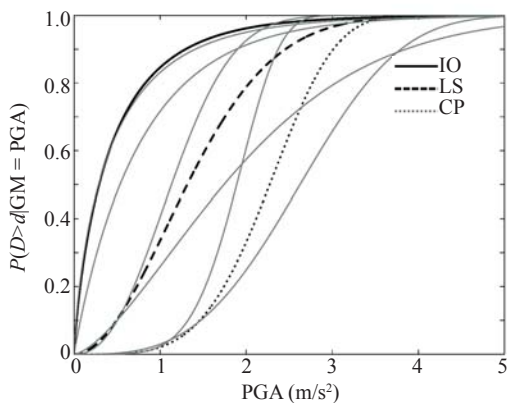


**Fig. 14** General fragility curves for substandard pre-seismic low rise RC buildings

## 6 Discussion and conclusions

A probabilistic analytical seismic fragility assessment framework is developed for low strength RC structures typical of developing countries. This framework is particularly applicable to fragility assessment of the brittle substandard RC structures failing in bond and shear. The complex degradation behaviour of substandard RC structures can be modelled through use of cyclic pushover curves, new capacity models and by using the modified capacity spectrum method which eliminates non-recoverable energy in the energy balance for maintaining true characteristics of degrading structure.

Secant period ( $T_{sec}$ ) values corresponding to each point on the capacity spectra are used as seismic demand parameter, since change in time period is a recognized global indicator of damage. Each capacity spectrum points are also assumed as a performance point associated with EEPP systems. A backward analysis technique is adopted to evaluate PGA using the modified capacity spectrum method based on FEMA 440 (MADRS). Mean values of Peak Ground Acceleration can be evaluated at every displacement interval corresponding to each performance point for the series of capacity curves for use in fragility curves.

The individual fragility curves corresponding to each sub-design and general fragility curves are derived to evaluate the POE of a particular damage state. The regression coefficients are defined to derive the mean and 90% confidence bound fragility curves. The proposed function and the regression coefficients may be adopted for developing typical fragility curves of low rise substandard RC structures of developing countries. Moreover, the fragility curves along with hazard curves can be integrated to evaluate the seismic risk of substandard RC structures, which are large proportion of RC building stock in developing countries.

## Acknowledgement

The first author acknowledges the scholarship provided by Higher Education Commission (HEC), Pakistan to conduct this research as a part of developing analytical seismic vulnerability assessment framework for reinforced concrete structures of developing countries. In addition, the second author also acknowledges the financial support provided by the Overseas Research Student (ORS) award scheme of the Vice-Chancellors' committee of the United Kingdom's universities as well as the A.G. Leventis Foundation.

## References

- Ahmad S (2011), "Seismic Vulnerability of Non-ductile Reinforced Concrete Structures in Developing Countries," *Ph.D Thesis*, The University of Sheffield, U.K.
- Ahmad S, Pilakoutas K, Neocleous K and Zaman Q U (2014), "Stress-strain Model for Low Strength Concrete in Uni-axial Compression," *Arabian Journal of Science and Engineering*, DOI: 10.1007/s13369-014-1411-1, Published Online Nov. 2014.
- Ahmed M (2006), "Earthquake Loss Estimation and Structural Vulnerability Assessment for Greater Cairo," *Ph.D Thesis*.
- ATC-40 (1996), *Seismic Evaluation and Retrofit of Concrete Buildings*, Publication of Applied Technology Council, Redwood City, California.
- Calvi GM (1999), "A Displacement-based Approach for Vulnerability Evaluation of Classes of Buildings," *Journal of Earthquake Engineering*, **3**: 411–438.
- Calvi GM, Pinho R and Crowley H (2006) "State-of-the-knowledge on the Period Elongation of RC Buildings during Strong Ground Shaking," *First European Conference on Earthquake Engineering and Seismology*, Geneva.
- Celik OC and Ellingwood BR (2008), "Modeling Beam-column Joints in Fragility Assessment of Gravity Load Designed Reinforced Concrete Frames," *Journal of Earthquake Engineering*, **12**: 357–381.
- Celik OC and Ellingwood BR (2010), "Seismic Fragilities for Non-ductile Reinforced Concrete Frames – role of Aleatoric and Epistemic Uncertainties," *Structural Safety*, **32**: 1–12.
- Cornell CA, Jalayer F, Hamburger RO and Foutch DA (2002), "Probabilistic Basis for 2000 sac Federal Emergency Management Agency Steel Moment Frame Guidelines," *Journal of Structural Engineering*, ASCE, **128**(4): 526–533.
- Crowley H, Pinho R and Bommer J (2004), "A Probabilistic Displacement-based Vulnerability Assessment Procedure for Earthquake Loss Estimation," *Bulletin of Earthquake Engineering*, **2**(2): 173–219.
- Dipasquale E and Cakmak AS (1988), "Identification of the Serviceability Limit State and Detection of Seismic Structural Damage," *Report NCEER-88-0022*, National Centre for Earthquake Engineering Research, State University of New York at Buffalo, NY.
- Dymiotis C, Kappos AJ and Chryssanthopoulos MK (1999), "Seismic Reliability of RC Frames with Uncertain Drift, and Member Capacity," *Journal of Structural Engineering*, ASCE, **125**(9): 1038–1047.
- Erberik MA (2008), "Fragility-based Assessment of Typical Mid-rise and Low-rise RC Buildings in Turkey," *Engineering Structures*, **30**: 1360–1374.
- Erberik MA and Elnashai AS (2005), "Seismic Vulnerability of Flat Slab Structures," *Technical Report*, Mid America Earthquake Centre, University of Illinois at Urbana-Champaign.
- FEMA356 (2000), *Prestandard and Commentary for the Seismic Rehabilitation of Buildings*, Federal Emergency Management Agency, Washington DC.
- FEMA440 (2005), *Improvement of Nonlinear Static Seismic Analysis Procedures*, Applied Technology Council (ATC-55 Project), Redwood City, California.
- Franchin P, Lupoi A, Pinto PE and Schotanus MIJ (2003), "Seismic Fragility of Reinforced Concrete Structures Using a Response Surface Approach," *Journal of Earthquake Engineering*, **7**(1) Special Issue: 45-77.
- Gardoni P, Mosalam KM and DerKiureghian A (2003), "Probabilistic Seismic Demand Models and Fragility Estimates for RC Bridges," *Journal of Earthquake Engineering*, **7**(1) Special Issue: 79–106.
- Kyriakides N (2008), "Seismic Vulnerability Assessment

of RC Buildings and Risk Assessment for Cyprus,” *Ph.D thesis*, The University of Sheffield.

Kyriakides N, Ahmad S, Pilakoutas K, Neocleous K and Chrysostomou C (2014), “A Probabilistic Analytical Seismic Vulnerability Assessment Framework for Substandard Structures in Developing Countries,” *Earthquake and Structures*, **6**(6): 665–687.

Kyriakides N, Pilakoutas K and Ahmad S (2012), “Vulnerability Curves for RC Substandard Buildings,” *15th World Conference on Earthquake Engineering (WCEE)*, Lisbon.

Lang K (2002), “Seismic Vulnerability of Existing Buildings,” *PhD thesis*, Swiss Federal Institute of Technology, Zurich.

Mander JB, Priestley MJN and Park R (1988), “Theoretical Stress-strain Model for Confined Concrete,” *Journal of Structural Engineering*, ASCE, **114**(8): 1804–1826.

McKay M, Conover W and Beckman R (1979), “A Comparison of Three Methods for Selecting Values of Input Variables in the Analysis of Output from a Computer Code,” *Technometrics*, **21**: 239–245.

Mosalam K, Ayala G, White R and Roth C (1997), “Seismic Fragility of RC Frames with and without Masonry Infill Walls,” *Journal of Earthquake Engineering*, **1**: 693–720.

Pinho R, Bommer JJ and Glaister S (2002), “A Simplified

Approach to Displacement-based Earthquake Loss Estimation Analysis,” *Proceedings of the 12th European Conference on Earthquake Engineering*, London, U.K., Paper No. 738.

Prakash V, Powell G and Campbell S (1994), “Drain-3d Base Program Description and User Guide, Version 1.10,” *Report No. UCB/SEMM-94/07*, Department of Civil Engineering, University of California, Berkeley.

Ramamoorthy S, Gardoni P and Bracci J (2006), “Probabilistic Demand Models and Fragility Curves for Reinforced Concrete Frames,” *Journal of Structural Engineering*, ASCE, **132**(10): 1563–1572.

Rossetto T and Elnashai AS (2005), “A New Analytical Procedure for the Derivation of Displacement-based Vulnerability Curves for Population of RC Structures,” *Engineering Structures*, **27**(3): 397–409.

Sezen H and Moehle JP (2004), “Shear Strength Model for Lightly Reinforced Concrete Columns,” *Journal of Structural Engineering*, ASCE, **130**(11): 1692–1703.

Singhal A and Kiremidjian A (1997), “A Method for Earthquake Motion-damage Relationships with Application to Reinforced Concrete Frames,” *NCEER Report NCEER-97-0008*, State University of New York at Buffalo, USA.

Zembaty Z, Kowalski M and Pospisil S (2006), “Dynamic Identification of an RC Frame in Progressive States of Damage,” *Engineering Structures*, **28**(5): 668–681.